# Role of the Helical Structure of the N-Terminal Region of Plasmodium falciparum Merozoite Surface Protein 2 in Fibril Formation and Membrane Interaction

**ARTICLE** *in* BIOCHEMISTRY · FEBRUARY 2012

Impact Factor: 3.02 · DOI: 10.1021/bi201880s · Source: PubMed

BIOCHEMISTRY
including biophysical chemistry & molecular biology

Article

pubs.acs.org/biochemistry

# Role of the Helical Structure of the N-Terminal Region of *Plasmodium falciparum* Merozoite Surface Protein 2 in Fibril Formation and Membrane Interaction

Xuecheng Zhang,*[,†] Christopher G. Adda,[‡] Andrew Low,[§] Jiahai Zhang,[∥] Wen Zhang,[∥] Hongbin Sun,[⊥] Xiaoming Tu,[∥] Robin F. Anders,[‡] and Raymond S. Norton[@]

[†]School of Life Sciences, Anhui University, Hefei, Anhui 230039, P. R. China

[‡]Department of Biochemistry, La Trobe University, Bundoora 3086, Australia

[§]The Walter and Eliza Hall Institute of Medical Research, Parkville 3052, Australia

[∥]School of Life Sciences, University of Science and Technology of China, Hefei, Anhui 230026, P. R. China

[⊥]High Magnetic Field Laboratory, Chinese Academy of Sciences, Hefei, Anhui 230088, P. R. China

[@]Monash Institute of Pharmaceutical Sciences, Monash University, Parkville 3052, Australia

Supporting Information

**ABSTRACT:** Merozoite surface protein 2 (MSP2), an abundant glycosylphosphatidylinositol-anchored protein on the surface of *Plasmodium falciparum* merozoites, is a promising malaria vaccine candidate. MSP2 is intrinsically disordered and forms amyloid-like fibrils in solution under physiological conditions. The 25 N-terminal residues ($MSP2_{1-25}$) play an important role in both fibril formation and membrane binding of the full-length protein. In this study, the fibril formation and solution structure of $MSP2_{1-25}$ in the membrane mimetic solvents sodium dodecyl sulfate (SDS), dodecylphosphocholine (DPC), and trifluoroethanol (TFE) have been investigated by transmission electronic microscopy, turbidity, thioflavin T fluorescence, circular dichroism (CD), and nuclear magnetic resonance (NMR) spectroscopy. Turbidity data showed that the aggregation of $MSP2_{1-25}$ was suppressed in the presence of membrane mimetic solvents. CD spectra indicated that helical structure in $MSP2_{1-25}$ was stabilized in SDS and DPC micelles and in high concentrations of TFE. The structure of $MSP2_{1-25}$ in 50% aqueous TFE, determined using NMR, showed that the peptide formed an amphipathic helix encompassing residues 10−24. Low concentrations of TFE favored partially folded helical conformations, as demonstrated by CD and NMR, and promoted $MSP2_{1-25}$ fibril formation. Our data suggest that partially folded helical conformations of the N-terminal region of MSP2 are on the pathway to amyloid fibril formation, while higher degrees of helical structure stabilized by high concentrations of TFE or membrane mimetics suppress self-association and thus inhibit fibril formation. The roles of the induced helical conformations in membrane interactions are also discussed.

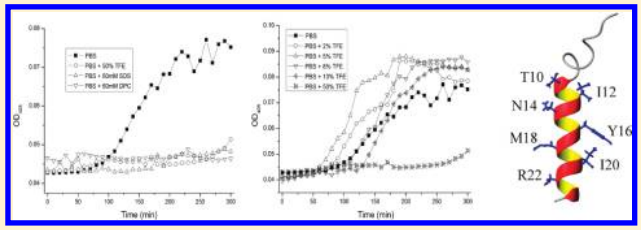


Malaria is one of the most important infectious diseases in the world, and the development of a vaccine against malaria is a major global health priority.[1] Merozoite surface protein 2 (MSP2), one of the most abundant proteins on the surface of malaria *Plasmodium falciparum* merozoites, has shown promise as a malaria vaccine component.[2−4] Recent studies demonstrated that full-length MSP2 is an intrinsically disordered protein (IDP), which is prone to forming amyloid fibrils.[5,6] There is also evidence that MSP2 exists in an oligomeric form on the merozoite surface,[6] but it is not known whether these oligomers are related to the amyloid fibrils formed by recombinant MSP2 in vitro. Understanding the propensity of MSP2 to aggregate in solution is important for its development as a vaccine candidate, as the soluble monomeric and fibrillar forms may have different antigenic and immunogenic properties.

The conserved N-terminal region of MSP2 ($MSP2_{1-25}$) constitutes the structural core of fibrils formed by full-length MSP2,[6] and peptides corresponding to both the entire conserved N-terminal region[7,8] and a centrally located fragment of this region[9] form fibrils similar to those formed by full-length MSP2. Nuclear magnetic resonance (NMR) experiments detected some local structure in $MSP2_{1-25}$ as a free peptide[7,8] and as part of full-length MSP2.[5] The observed amide proton chemical shifts indicated that this region assumes a conformation in the isolated peptide similar to its conformation in the full-length recombinant protein.[5] The N-terminal region of the protein is also essential for the interaction of the recombinant FC27 isoform of MSP2 with dodecylphosphocholine (DPC) lipid micelles.[5]

Many intrinsically disordered amyloidogenic proteins, including α-synuclein,[10] Aβ,[11] and tau,[12] contain some residual structures in

**Received:** December 19, 2011
**Revised:** January 19, 2012
**Published:** January 23, 2012

solution and are able to form helical structure upon binding to membranes.[13−15] Moreover, membrane binding of these amyloidogenic proteins can alter their aggregation processes.[16,17] Membrane binding accompanied by conformational change and aggregation of these proteins may also disrupt membranes and thereby contribute to the pathological changes that lead to serious diseases such as Parkinson's, Alzheimer's, and prion diseases that are accompanied by amyloid deposition.[18−20]

Sodium dodecyl sulfate (SDS) and DPC micelles are often used as membrane mimetics for in vitro studies.[21] Trifluoroethanol (TFE) has also been widely used to mimic membrane environments when peptides are not structured in water and only poorly structured in phospholipid micelles,[22−24] with low concentrations mimicking the proximity to the membrane and higher concentrations mimicking surface and interior environments.[25,26] In our study, we have used transmission electronic microscopy (TEM), thioflavin T (ThT) binding fluorescence, turbidity, circular dichroism, and NMR spectroscopy to investigate the fibril formation and solution structure of $MSP2_{1-25}$ in the presence of SDS and DPC micelles and in aqueous TFE. We show that $MSP2_{1-25}$ forms substantial helical structures in membrane environments, which alter the fibril formation to different degrees. Our results imply that partial helical conformations are on-pathway intermediates leading to $MSP2_{1-25}$ aggregation and fibril formation.

## MATERIALS AND METHODS

**Materials.** TFE and ThT were purchased from Sigma-Aldrich (Shanghai, P. R. China). $^2H_2O$ and TFE-$^2H_2$ were from Cambridge Isotope Laboratories. DPC was obtained from Anatrace Inc. Other reagents were all of analytical or higher purity.

$MSP2_{1-25}$ (98% pure) was purchased from GL Biochem Ltd. (Shanghai, P. R. China) and used without further purification. Peptide solutions were prepared by dissolving the peptide in Milli-Q water at a concentration of 5 mg/mL and incubating the solution at 80 °C for 10 min, followed by centrifugation at 12000 rpm for 10 min to remove insoluble particles. The exact concentrations of peptide in the final stock solutions were determined by absorption at 280 nm using an extinction coefficient of 2980 $M^{-1}$ $cm^{-1}$, which was calculated from the amino acid composition using the ProtParam program in ExPasy (http://www.expasy.ch/tools/#primary).

**Transmission Electron Microscopy.** Samples for TEM were prepared as for the ThT fluorescence assay (see below) except that they contained no ThT and were left stationary at room temperature (20 °C) until they were examined by TEM. Ten microliters of each sample was deposited on a carbon-coated grid; excess material was removed by blotting, and samples were negatively stained twice with 10 μL of a 2% uranyl acetate solution (w/v). The grids were air-dried and viewed on a JEM-2100 (JEOL) transmission electron microscope.

**ThT Binding Fluorescence and Turbidity.** A stock solution of 500 μM ThT was prepared in Milli-Q water and stored at 4 °C protected from light to prevent quenching. For ThT fluorescence measurements, 200 μL solutions containing 10 μM ThT and 20−40 μM $MSP2_{1-25}$ were incubated in 96-microwell black polystyrene plates with flat bottoms (Costar, Corning Inc.) and measured at various time intervals. Three replicates corresponding to three wells were measured for each sample to allow for well-to-well variation. A SpectraMax M5 multidetection reader (Molecular Devices Ltd.) was used to read the ThT fluorescence with excitation at 443 nm and emission at 484 nm. Both excitation and emission slits were maintained at 2 nm. All measurements were taken at 20 °C.

The samples for turbidity measurements were prepared in the same way but were set up in 96-microwell clear polystyrene plates with flat bottoms (Greiner), allowing the measurement of absorption at 405 nm.

**Circular Dichroism.** Circular dichroism measurements were conducted on a Jasco model J-810 spectropolarimeter. Spectra were recorded in the range of 190−260 nm at a protein concentration of 30 or 90 μM (0.1 or 0.3 mg/mL, respectively) using a 0.1 cm path-length cell. All CD measurements were performed at room temperature (20 °C), and each spectrum was the average of three scans smoothed for further analysis. The data averaging and smoothing operations were performed using the function provided in the spectral analysis software of the spectrometer.

**NMR Spectroscopy.** NMR measurements were taken at 25 °C on a Bruker DMX-500 spectrometer. Samples (500 μL) of 1.3 mM $MSP2_{1-25}$ were prepared in water containing 10% $^2H_2O$, without any TFE, or with 5 or 50% TFE-$^2H_2$. NOESY spectra were recorded with mixing times of 200 ms, and TOCSY experiments were conducted with spin-lock times of 80 ms. The data sizes for the NOESY, TOCSY, and DQF-COSY experiments were 512 ($t_1$) × 2K ($t_2$) points. All spectra were acquired in TPPI mode. The carrier frequency was centered on the $H_2O$ resonance, and $^1H$ chemical shifts were referenced to water at 298 K (4.773 ppm). The strong solvent resonance was suppressed using the Watergate sequence[27] during the preparation period for TOCSY and DQF-COSY experiments, and also during the mixing time for the NOESY experiments. NMR data were processed and analyzed using NMRPipe[28] and Sparky.[29] Data were typically apodized using a shifted sin or $sin^2$ function before zero-filling and Fourier transformation in both dimensions.

Structure calculations were conducted with CNS[30] employing a simulated annealing protocol for torsion angle dynamics, with upper boundaries of 2.8, 3.5, and 5.0 Å and a lower boundary of 1.80 Å on the basis of NOE intensity measurements. For the initial rounds of structure calculations, only unambiguous NOEs were used. Subsequently, all other ambiguous NOEs were introduced in consecutive steps. Simple nonbonded interactions were used during structure calculations. At the final stage, 100 structures were calculated, from which the 10 structures with the lowest energy were selected. The calculated structures were evaluated using PROCHECK_NMR[31] and MOLMOL.[32]

## RESULTS

**$MSP2_{1-25}$ Was Prone to Aggregation under Physiological Conditions, and the Aggregation Was Suppressed under Membrane Mimetic and Acidic Conditions.** In PBS, $MSP2_{1-25}$ aggregated readily to form fibrils, as demonstrated by TEM (Figure 1) and ThT binding (Figure 2A). The sigmoidal increase in ThT fluorescence indicated a nucleation-dependent aggregation process, which is typical of amyloid fibril formation. Because ThT added to preformed $MSP2_{1-25}$ aggregates gave a very weak ThT fluorescence signal in the presence of SDS and DPC micelles or a high concentration (50%) of TFE (Figure S1, Supporting Information), ThT was not suitable for monitoring the kinetics of formation of fibrils by the MSP2 peptide under these conditions. Measurements of solution turbidity were therefore used to assess the influence of these three membrane mimetic solvents on the aggregation dynamics of $MSP2_{1-25}$. The results showed that

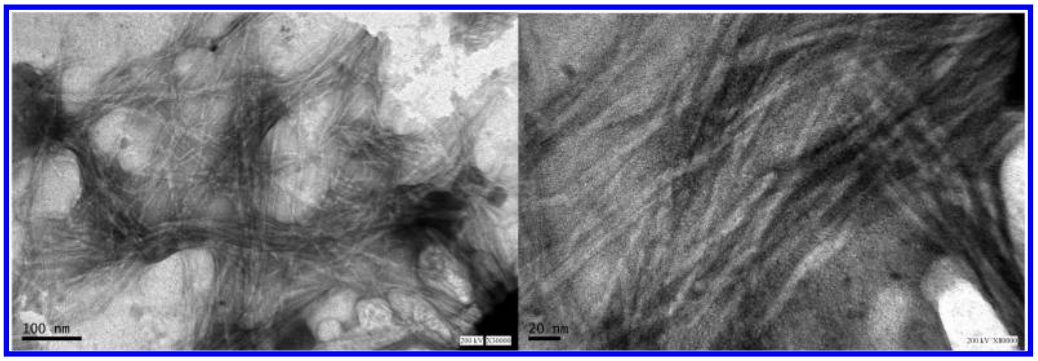


**Figure 1.** TEM diagrams for the fibrils formed by $MSP2_{1-25}$ in PBS. The samples were prepared and manipulated as described for the ThT fluorescence assay, except that the former contained no ThT. After fluorescence kinetics measurements, the samples were left stationary at room temperature (20 °C) for 1 day until they were examined by TEM.

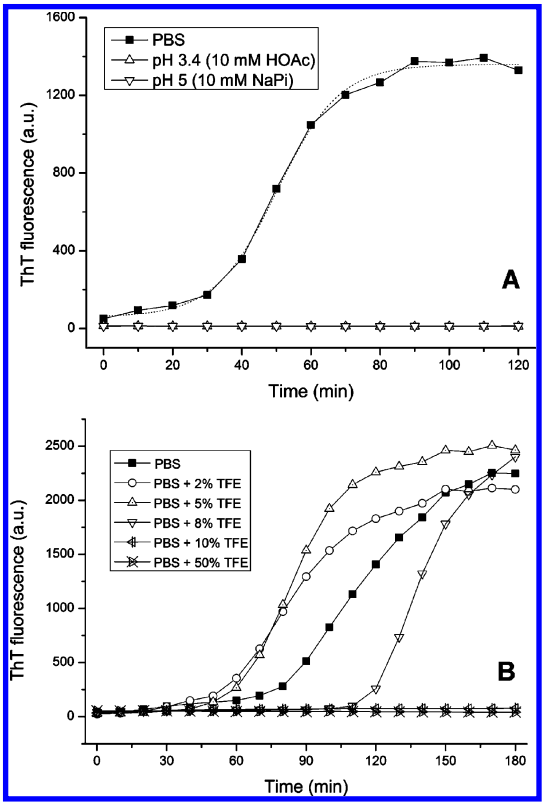


**Figure 2.** Fibril formation kinetics of $MSP2_{1-25}$ (A) at neutral pH and acidic pH and (B) in PBS in the presence of different concentrations of TFE, monitored by ThT binding fluorescence. The concentrations of the peptide and ThT were ~30 and ~10 $\mu$M, respectively. The dotted line represents the fitted sigmoidal line for the PBS data.

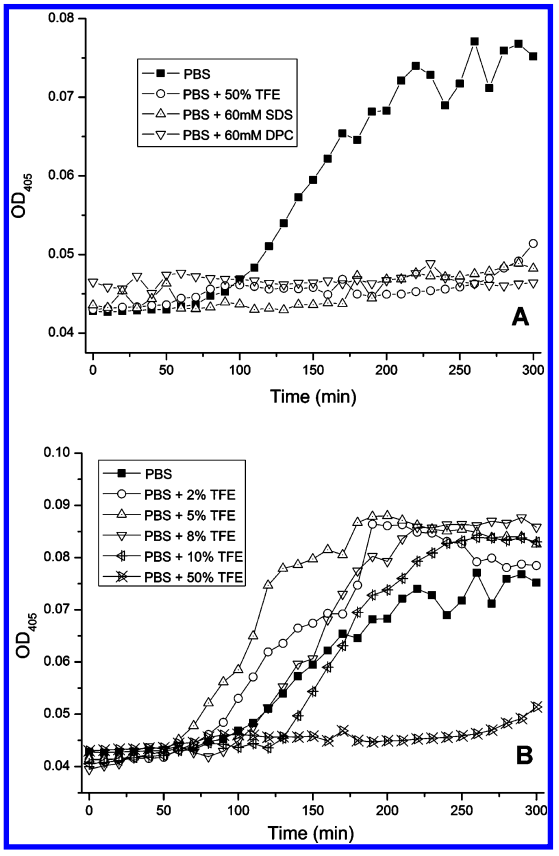


**Figure 3.** (A) Fibril formation kinetics of $MSP2_{1-25}$ in PBS, PBS with 60 mM SDS, PBS with 60 mM DPC, and PBS with 50% TFE, monitored via turbidity at 405 nm. (B) Influence of different concentrations of TFE on $MSP2_{1-25}$ fibril formation in PBS, monitored via turbidity at 405 nm. The concentrations of the peptide and ThT were ~30 and ~10 $\mu$M, respectively.

adding the three membrane mimetic solvents strongly suppressed the aggregation of $MSP2_{1-25}$ (Figure 3A). Examination of these samples by TEM was complicated by artifacts introduced by the presence of these membrane mimetics, but it was clear that fibril formation was not totally suppressed except by 60 mM DPC (Figure S2, Supporting Information).

The aggregation of $MSP2_{1-25}$ under physiological conditions prevented further investigation of the solution structure of the peptide using CD and NMR. To circumvent this, acidic conditions (10 mM HOAc at pH 3.4 or 10 mM $NaP_i$ at pH 5), which significantly inhibited aggregation of $MSP2_{1-25}$ (Figure 2A) while preserving structure similar to that at physiological pH[8] (Figure S3, Supporting Information), were employed for the structural studies. TEM studies of samples of $MSP2_{1-25}$ in acidic buffers showed there were few aggregates formed in the presence or absence of the three membrane mimetic solvents under these conditions (data not shown).

**Low Concentrations of TFE Promoted $MSP2_{1-25}$ Aggregation, while High Concentrations Suppressed Aggregation.** As the fluorescence of ThT bound to $MSP2_{1-25}$ aggregates was not markedly affected by concentrations of TFE much lower than 50%, it was feasible to use ThT fluorescence to investigate the influence of these lower concentrations of TFE on the kinetics of $MSP2_{1-25}$ aggregation. Whereas high


dx.doi.org/10.1021/bi201880s | *Biochemistry* 2012, 51, 1380−1387

concentrations of TFE strongly suppressed the aggregation of $MSP2_{1-25}$, low concentrations showed the opposite effect. At concentrations below 8%, TFE enhanced $MSP2_{1-25}$ aggregation, with a clear shortening of the nucleation phase (Figure 2B). When the concentration of TFE increased beyond 10%, the aggregation of $MSP2_{1-25}$ was significantly delayed, with the ThT fluorescence remaining low (Figure 2B). These concentration-dependent and opposite effects of TFE on the kinetics of $MSP2_{1-25}$ aggregation were confirmed by turbidity measurements (Figure 3B). The apparent difference between the effects of low concentrations of TFE in Figures 2B and 3B may reflect the fact that ThT is sensitive to cross-$\beta$ structure while turbidity is sensitive to aggregate size. Our results are consistent with a fibrillation mechanism in which peptides form intermediates rich in helical structure prior to their transformation to fibrils rich in cross-$\beta$ structure.

**SDS and DPC Micelles and High Concentrations of TFE Induced $MSP2_{1-25}$ To Form Substantial Helical Structure.** $MSP2_{1-25}$ was largely disordered in aqueous solution at both neutral and acidic pH as indicated by the significant negative peak around 200 nm in CD spectra (Figure 4A). This was consistent with previously published CD and NMR data for $MSP2_{1-25}$ in aqueous solution.[5,7,8] Poor chemical shift dispersion in the one-dimensional (1D) $^1$H NMR spectrum

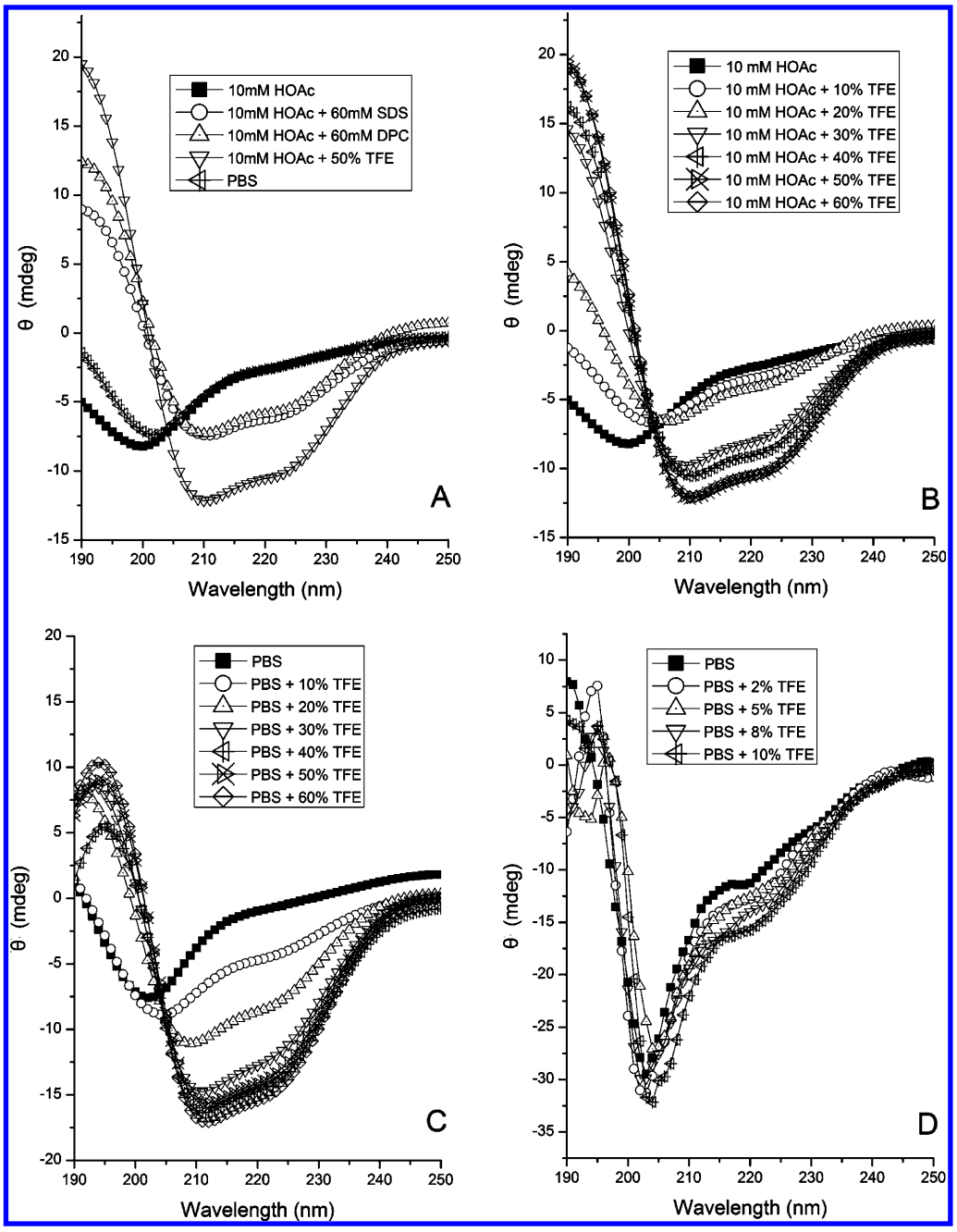


**Figure 4.** Circular dichroism spectra of $MSP2_{1-25}$ (A) in aqueous and membrane mimetic solutions, (B) at pH 3.4 (in 10 mM HOAc) with different concentrations of TFE, and (C and D) at neutral pH (in PBS) with different concentrations of TFE, demonstrating the disordered conformations of the peptide in aqueous solutions and the stabilization of helical structure in the presence of membrane mimetic solvents. The concentrations of the peptide were ~30 $\mu$M for panels A–C and 80 $\mu$M for panel D. The curves in panel A for acetate and phosphate buffers are superimposed, as are those for the peptide in SDS and DPC. In panel B, the curves for 50 and 60% TFE are completely overlapped.


dx.doi.org/10.1021/bi201880s | *Biochemistry* 2012, 51, 1380–1387

(data not shown) was also consistent with the largely disordered nature of $MSP2_{1-25}$.[8]

In the presence of 60 mM SDS or DPC micelles, $MSP2_{1-25}$ adopted conformations with substantial helical structure, as indicated by troughs around 208 and 222 nm in CD spectra (Figure 4A). Increasing the concentrations of SDS and DPC (to 200 mM) had no further effect on the CD spectra (data not shown). TFE also induced $MSP2_{1-25}$ to form helical structure (Figure 4A,B), with the helical content reaching a maximum at approximately 50% TFE (Figure 4B). The extents of helical structure induced by SDS and DPC micelles were similar (26.2 and 24.3%, respectively, calculated with the Yang method[33]) but less than that induced by 50% TFE (31.2%). Although the peptide aggregated rapidly at neutral pH, corresponding CD experiments under physiological conditions (in PBS) were performed for comparison. The results obtained (Figure 4C) were similar to those found in 10 mM HOAc, confirming the relevance of studies under acidic conditions.

**Low Concentrations of TFE Promoted Some Helical Structure in $MSP2_{1-25}$.** CD measurements performed on $MSP2_{1-25}$ in PBS in the presence of the low concentrations of TFE (<10%) that promoted aggregation showed an increase in helical content, as was found for higher, inhibitory, concentrations of TFE. This was demonstrated by the deepening of the trough at 222 nm in the CD spectra as the TFE concentration was increased from 0 to 2, 5, 8, and 10% (Figure 4D).

This nascent helical structure in low concentrations of TFE was confirmed by NMR data. As in PBS, $MSP2_{1-25}$ in a sodium phosphate solution at pH 5 aggregated eventually, but after a much longer nucleation phase (Figure 2), which made NMR analysis of the $MSP2_{1-25}$ samples feasible under these conditions. COSY, TOCSY, and NOESY spectra were recorded for 1 mM $MSP2_{1-25}$ in 10 mM $NaP_i$ with and without 5% TFE. Chemical shifts of $C^{\alpha}H$ resonances in particular are indicative of the secondary structures of peptides and proteins,[34,35] with $C^{\alpha}H$ resonances from helical regions generally being upfield of their random coil values.[36] As shown in Figure 5, $MSP2_{1-25}$ in 10 mM

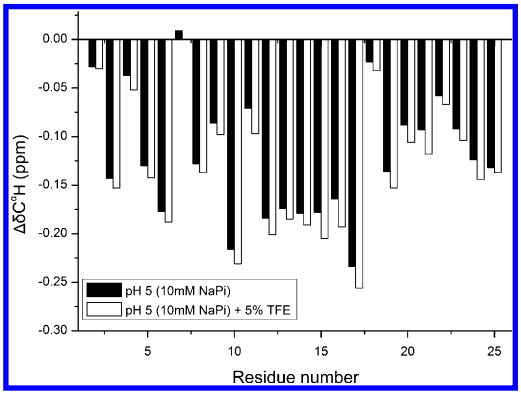


**Figure 5.** Chemical shift deviations from random coil values[36] for $C^{\alpha}H$ chemical shifts of $MSP2_{1-25}$ in 10 mM $NaP_i$ at pH 5 with and without 5% TFE. The negative deviations imply a propensity to form helical structure.

$NaP_i$ at pH 5 showed an enhanced propensity to form helical structure in the presence of 5% TFE, as illustrated by the more pronounced upfield $C^{\alpha}H$ resonances.

**Structure of $MSP2_{1-25}$ in 50% TFE in 10 mM HOAc.** Although SDS and DPC micelles induced helical structures in $MSP2_{1-25}$ and suppressed fibril formation by the peptide to some extent, these detergent solutions were less suited for structural studies of the peptide under membrane mimetic conditions by NMR spectroscopy. The 1D $^1H$ NMR spectrum of the peptide in SDS and 10 mM HOAc displayed broad resonances (Figure S4, Supporting Information), which might have resulted from conformational exchange between the free and detergent-bound peptide. The 1D $^1H$ NMR spectrum of $MSP2_{1-25}$ in DPC and 10 mM HOAc gave better resolved resonances (Figure S5, Supporting Information), but with intensities that decreased to less than half within a few hours.

CD data (Figure 4) suggested that 50% TFE was sufficient to stabilize the highest content of helical structure in $MSP2_{1-25}$. In addition, the 1D $^1H$ NMR spectrum gave reasonably well-resolved resonances (Figure S6, Supporting Information) and was stable in HOAc but not PBS for many weeks, which was necessary for two-dimensional NMR studies. For these reasons, 50% TFE in 10 mM HOAc was chosen as the solvent for determination of the solution structure of $MSP2_{1-25}$ in a membrane mimetic environment.

The $^1H$ NMR resonances of $MSP2_{1-25}$ were assigned using a combination of DQF-COSY, TOCSY, and NOESY spectra.[37] Figure S7A of the Supporting Information shows some of the NOEs in the NH−NH region of a 200 ms NOESY spectrum of $MSP2_{1-25}$ in 50% TFE and 10 mM HOAc, and Figure S7B of the Supporting Information shows the $d_{\alpha N}(i,i+1)$ NOE connectivities. NMR resonance assignments are documented in Table S1 of the Supporting Information.

Comparison of the $C^{\alpha}H$ chemical shifts of $MSP2_{1-25}$ in 50% TFE with "random coil" reference values[36] (Figure 6A) shows

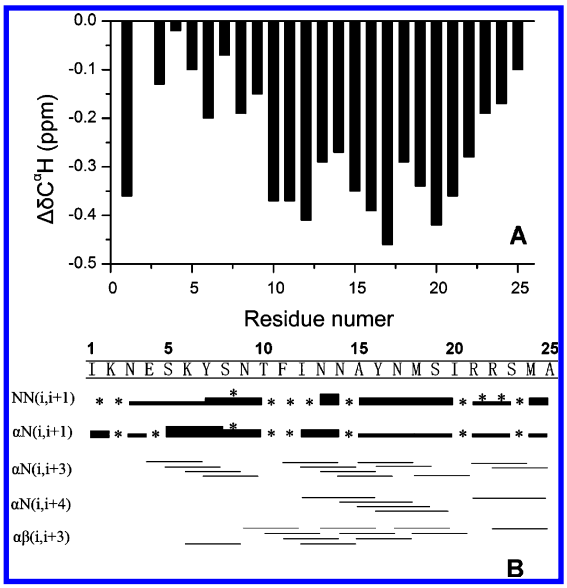


**Figure 6.** (A) Chemical shift deviations from random coil values[36] for $C^{\alpha}H$ shifts of $MSP2_{1-25}$ in 50% TFE in 10 mM HOAc, implying the propensity to form helical structure along the peptide and relatively rigid helix in the range of residues 10−24. (B) Sequential and medium-range NOEs for $MSP2_{1-25}$ in 50% TFE in 10 mM HOAc, demonstrating characteristic NOEs for helical structures.[37] The thickness of the bars indicates the relative intensity of the resonances, and the asterisks signify the NOEs whose existence or intensity is ambiguous because of resonance overlap.

upfield deviations for all residues in the peptide, consistent with the helical structure indicated by CD. The $C^{\alpha}H$ shifts of residues 10−22 exhibited relatively greater deviations than those from the N-terminal region, implying more stable helical


dx.doi.org/10.1021/bi201880s | Biochemistry 2012, 51, 1380−1387

structure in this region. These conclusions are supported by the pattern of medium-range NOEs, with many $d_{\alpha N}(i,i+3)$, $d_{\alpha N}(i,i+4)$, and $d_{\alpha\beta}(i,i+3)$ NOEs in the region of residues 10−25 (Figure 6B), signifying a regular helix structure. The weaker sequential $d_{NN}(i,i+1)$ and stronger $d_{\alpha N}(i,i+1)$ for residues 2−10 imply a relatively more extended conformation in this region, consistent with the lack of intermediate and long-range NOEs at the N-terminus.

A total of 100 structures of $MSP2_{1-25}$ in 10 mM HOAc and 50% TFE were generated by restrained molecular dynamics and distance geometry-simulated annealing calculations in CNS,[30] and the 10 structures with the lowest potential energy were selected for further examination. The structural statistics are summarized in Table 1. Most of the dihedral angles were found in the most favored or additionally allowed regions of the Ramachandran plot, indicating the good quality of the structures. As shown in Figure 7A, the structure consists of a regular $\alpha$-helix in the region of residues 10−24, with an extended conformation for residues 5−9 and a disordered N-terminus. The helical structure is moderately amphipathic, with all three hydrophobic side chains in this region located on one side of the $\alpha$-helix and polar and charged side chains on the other (Figure 7B). The amphipathic nature of the $\alpha$-helix formed by $MSP2_{1-25}$ is further illustrated by the surface distribution of charge on the average structure shown in Figure 7C.

**Table 1. Summary of Structural Statistics of $MSP2_{1-25}$ in 50% TFE and 10 mM HOAc at 25 °C**

| | |
|---|---|
| no. of nonredundant distance restraints | 388 |
| intraresidue ($i = j$) | 235 |
| sequential ($\|i - j\| = 1$) | 95 |
| short-range ($1 < \|i - j\| < 5$) | 58 |
| long-range ($\|i - j\| > 5$) | 0 |
| deviations from ideal geometry | |
| bond lengths (Å) | 0.0044 ± 0.00002 |
| bond angles (deg) | 0.442 ± 0.0038 |
| impropers (deg) | 0.1539 ± 0.0105 |
| rmsd over all residues[a] | |
| all heavy atoms (Å) | 2.42 ± 0.50 |
| backbone heavy atoms (N, $C^{\alpha}$, C′) (Å) | 1.55 ± 0.54 |
| rmsd for the helical region[b] | |
| all heavy atoms (Å) | 1.59 ± 0.29 |
| backbone heavy atoms (N, $C^{\alpha}$, C′) (Å) | 0.54 ± 0.14 |
| Ramachandran plot[c] (%) | |
| most favored | 89.1 |
| allowed | 9.6 |
| additionally allowed | 1.3 |
| disallowed | 0 |

[a]Root-mean-square deviation (rmsd) values from MOLMOL. [b]Over residues 10−24. [c]Data from PROCHECK_NMR.

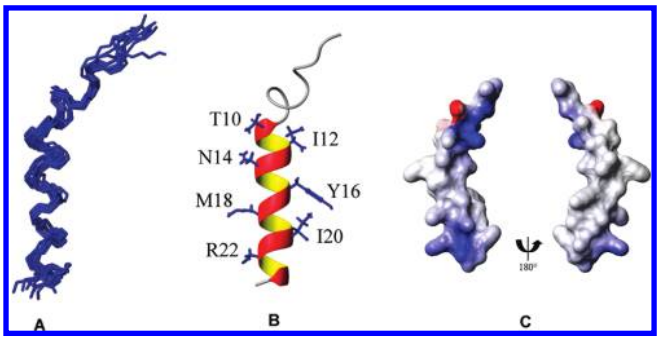


**Figure 7.** (A) Structure of $MSP2_{1-25}$ in 50% TFE in 10 mM HOAc (superimposed over the backbone N, C$\alpha$, and carbonyl C atoms of all residues). (B) Average of the 10 lowest-energy structures of $MSP2_{1-25}$ in 50% TFE in 10 mM HOAc, with hydrophobic side chains and polar side chains shown on the opposite sides. (C) Surface representation of the average structure of $MSP2_{1-25}$ in 50% TFE in 10 mM HOAc, with positive charge colored blue and negative charge red. All structures are shown with the N-terminus at the top.

## DISCUSSION

MSP2 is an abundant *P. falciparum* merozoite surface protein, which may play a role in the initial interaction of the merozoite with the host erythrocyte. Understanding the interactions of MSP2 with both the parasite and erythrocyte membranes is therefore of interest. We have shown previously that MSP2 can bind to DPC micelles and that the conserved 25-residue N-terminal region is important for this interaction.[5] This region of MSP2 is also responsible for the formation of amyloid-like fibrillar aggregates,[6] and for these reasons, we have investigated the structure of $MSP2_{1-25}$ and its aggregation under membrane mimetic conditions.

Numerous studies have demonstrated that the fibril formation kinetics of amyloidogenic proteins or peptides are modified when they associate with membranes or lipids.[16,17] For example, a lipid bilayer facilitated nucleation of A$\beta$ fibrils,[38] anionic phospholipids enhanced fibrillogenesis of $\alpha$-synuclein,[39] and anionic micelles and vesicles induced fibril formation by tau.[40] In contrast, other studies showed that lipids inhibited aggregation of $\alpha$-synuclein,[41] insulin,[42] and A$\beta$ peptide.[43] Our results indicated that both SDS and DPC micelles inhibit the aggregation of $MSP2_{1-25}$, although not completely as some fibrils were seen in negatively stained preparations of $MSP2_{1-25}$ in SDS examined by TEM. 1D NMR data showed broadened or attenuated resonances for the peptide in SDS or DPC; as the mass of the complex of monomeric $MSP2_{1-25}$ with DPC or SDS micelles is less than 20 kDa, the overall tumbling of the micelle-bound peptide should not have been a problem for high-resolution NMR studies, so the broadening and attenuation of resonances in the micelles presumably result from conformational exchange or/and the formation of aggregates.

$MSP2_{1-25}$, which is the core of the amyloid-like fibrils formed by recombinant MSP2,[6] was shown previously to have some helix propensity in NMR studies of the full-length protein.[5] The results of our CD and NMR studies with the peptide in SDS and DPC micelles, and 50% TFE, showed that this nascent helix was stabilized under these membrane mimetic conditions. This stabilization was more marked for residues 10−24, which form a regular $\alpha$-helix in 50% TFE, with residues 5−9 adopting an extended conformation and the N-terminus being disordered. Stabilization of the helix, which would decrease the probability of a conformational change to $\beta$-strand, was most likely responsible for inhibition of the aggregation of $MSP2_{1-25}$ into fibrils at higher TFE concentrations.

Recent evidence indicates that $\alpha$-helical species are important intermediates on the pathway to the formation of amyloid fibrils[44−46] and that conformational changes resulting in increased $\beta$-sheet content occur subsequently. Our results support such a model for formation of fibrils by $MSP2_{1-25}$. At TFE concentrations of <10%, a small but reproducible increase in the kinetics of fibril formation as measured by ThT fluorescence was observed. Correspondingly, CD and NMR analyses showed an increased helical content at these low TFE concentrations. The involvement in formation of fibrils of MSP2 conformers


dx.doi.org/10.1021/bi201880s | *Biochemistry* 2012, 51, 1380−1387

containing some helical structure in the N-terminally conserved region of the protein is consistent with the many observations that the formation of more ordered regions of structure facilitates formation of fibrils by other intrinsically disordered proteins.[45,47−49] If some α-helix promotes fibril formation but greater α-helix stabilization inhibits aggregation, we might expect that the kinetics of formation of fibrils by MSP2 would vary markedly under different conditions. We have reported previously that the kinetics of fibril formation by 3D7 MSP2 are very much slower than the kinetics of fibril formation by FC27 MSP2.[6] The $MSP2_{1-25}$ sequence is common to these two isoforms of MSP2, but the propensity for α-helix formation in this region, and hence the propensity to form fibrils, may be influenced by the very different sequences in the variable region immediately C-terminal to $MSP2_{1-25}$.

The helical contents of $MSP2_{1-25}$ induced by SDS and DPC were lower than in 50% TFE, which may be a consequence of exchange between the lipid-bound and water-soluble states in these micelles, representing the state of the peptide prior to binding to or insertion into a membrane. The conformation of the peptide in 50% TFE, with more pronounced helical structure, presumably represents the state of the peptide bound to or within a membrane, suggesting a possible mechanism by which MSP2 may undergo conformational changes during the process of merozoite attachment and invasion. Gaining an understanding of the ways in which this GPI-anchored parasite antigen is more ordered than recombinant monomeric MSP2 in solution will be important for the further development of MSP2 as a component of a malaria vaccine. The association with membranes may also serve to limit aggregation of MSP2 on the parasite surface. More generally, the N-terminal region of MSP2 represents another example of a highly unstructured region of a protein whose propensity for fibril formation is enhanced by low levels of helical stabilization and disfavored by more substantial helical stabilization.

## ■ ASSOCIATED CONTENT

### Ⓢ Supporting Information

Seven figures and one table. This material is available free of charge via the Internet at http://pubs.acs.org.

## ■ AUTHOR INFORMATION


### Corresponding Author

*E-mail: turenzh@ahu.edu.cn. Telephone: 86 551 5107341. Fax: 86 551 5107354.



### Funding

This work was supported in part by grants to X.Z. from the Anhui Provincial Natural Science Foundation (Grant 090413079) and the Scientific Research Foundation for Returned Scholars, Ministry of Education of China, and to R.S.N. and R.F.A. from the National Health and Medical Research Council (NHMRC) of Australia (Grant 637368). R.S.N. acknowledges fellowship support from the NHMRC.


### Notes

The authors declare no competing financial interest.

## ■ ACKNOWLEDGMENTS


We thank Dr. F. Delaglio and Prof. A. Bax for providing NMRPipe and Prof. T. D. Goddard and Prof. D. G. Kneller for providing Sparky.


## ■ ABBREVIATIONS

CD, circular dichroism; COSY, correlation spectroscopy; DPC, dodecylphosphocholine; $MSP2_{1-25}$, residues 1−25 of merozoite surface protein 2; NMR, nuclear magnetic resonance; NOE, nuclear Overhauser effect; NOESY, nuclear Overhauser effect spectroscopy; SDS, sodium dodecyl sulfate; TEM, transmission electronic microscopy; TFE, trifluoroethanol; ThT, thioflavin T; TOCSY, total correlated spectroscopy.

## ■ REFERENCES


(1) Snow, R. W., Guerra, C. A., Noor, A. M., Myint, H. Y., and Hay, S. I. (2005) The global distribution of clinical episodes of *Plasmodium falciparum* malaria. *Nature 434*, 214−217.

(2) Genton, B., Al-Yaman, F., Betuela, I., Anders, R. F., Saul, A., Baea, K., Mellombo, M., Taraika, J., Brown, G. V., Pye, D., Irving, D. O., Felger, I., Beck, H. P., Smith, T. A., and Alpers, M. P. (2003) Safety and immunogenicity of a three-component blood-stage malaria vaccine (MSP1, MSP2, RESA) against *Plasmodium falciparum* in Papua New Guinean children. *Vaccine 22*, 30−41.

(3) McCarthy, J. S., Marjason, J., Elliott, S., Fahey, P., Bang, G., Malkin, E., Tierney, E., Aked-Hurditch, H., Adda, C., Cross, N., Richards, J. S., Fowkes, F. J., Boyle, M. J., Long, C., Druilhe, P., Beeson, J. G., and Anders, R. F. (2011) A phase 1 trial of MSP2-C1, a blood-stage malaria vaccine containing 2 isoforms of MSP2 formulated with Montanide® ISA 720. *PLoS One 6*, e24413.

(4) Anders, R. F., Adda, C. G., Foley, M., and Norton, R. S. (2010) Recombinant protein vaccines against the asexual blood stages of *Plasmodium falciparum*. *Hum. Vaccines 6*, 39−53.

(5) Zhang, X., Perugini, M. A., Yao, S., Adda, C. G., Murphy, V. J., Low, A., Anders, R. F., and Norton, R. S. (2008) Solution conformation, backbone dynamics and lipid interactions of the intrinsically unstructured malaria surface protein MSP2. *J. Mol. Biol. 379*, 105−121.

(6) Adda, C. G., Murphy, V. J., Sunde, M., Waddington, L. J., Schloegel, J., Talbo, G. H., Vingas, K., Kienzle, V., Masciantonio, R., Howlett, G. J., Hodder, A. N., Foley, M., and Anders, R. F. (2009) *Plasmodium falciparum* merozoite surface protein 2 is unstructured and forms amyloid-like fibrils. *Mol. Biochem. Parasitol. 166*, 159−171.

(7) Low, A., Chandrashekaran, I. R., Adda, C. G., Yao, S., Sabo, J. K., Zhang, X., Soetopo, A., Anders, R. F., and Norton, R. S. (2007) Merozoite surface protein 2 of *Plasmodium falciparum*: Expression, structure, dynamics, and fibril formation of the conserved N-terminal domain. *Biopolymers 87*, 12−22.

(8) Yang, X., Adda, C. G., Keizer, D. W., Murphy, V. J., Rizkalla, M. M., Perugini, M. A., Jackson, D. C., Anders, R. F., and Norton, R. S. (2007) A partially structured region of a largely unstructured protein, *Plasmodium falciparum* merozoite surface protein 2 (MSP2), forms amyloid-like fibrils. *J. Pept. Sci. 13*, 839−848.

(9) Yang, X., Adda, C. G., MacRaild, C. A., Low, A., Zhang, X., Zeng, W., Jackson, D. C., Anders, R. F., and Norton, R. S. (2010) Identification of key residues involved in fibril formation by the conserved N-terminal region of *Plasmodium falciparum* merozoite surface protein 2 (MSP2). *Biochimie 92*, 1287−1295.

(10) Sung, Y. H., and Eliezer, D. (2007) Residual structure, backbone dynamics, and interactions within the synuclein family. *J. Mol. Biol. 372*, 689−707.

(11) Lim, K. H., Collver, H. H., Le, Y. T., Nagchowdhuri, P., and Kenney, J. M. (2007) Characterizations of distinct amyloidogenic conformations of the Aβ (1−40) and (1−42) peptides. *Biochem. Biophys. Res. Commun. 353*, 443−449.

(12) Mukrasch, M. D., Bibow, S., Korukottu, J., Jeganathan, S., Biernat, J., Griesinger, C., Mandelkow, E., and Zweckstetter, M. (2009) Structural polymorphism of 441-residue tau at single residue resolution. *PLoS Biol. 7*, e34.

(13) Shao, H., Jao, S., Ma, K., and Zagorski, M. G. (1999) Solution structures of micelle-bound amyloid β-(1−40) and β-(1−42) peptides of Alzheimer's disease. *J. Mol. Biol. 285*, 755−773.

(14) Nagarajan, S., Ramalingam, K., Neelakanta Reddy, P., Cereghetti, D. M., Padma Malar, E. J., and Rajadas, J. (2008) Lipid-induced conformational transition of the amyloid core fragment Aβ(28−35) and its A30G and A30I mutants. *FEBS J. 275*, 2415−2427.
(15) Georgieva, E. R., Ramlall, T. F., Borbat, P. P., Freed, J. H., and Eliezer, D. (2008) Membrane-bound α-synuclein forms an extended helix: Long-distance pulsed ESR measurements using vesicles, bicelles, and rodlike micelles. *J. Am. Chem. Soc. 130*, 12856−12857.
(16) Gorbenko, G. P., and Kinnunen, P. K. (2006) The role of lipid-protein interactions in amyloid-type protein fibril formation. *Chem. Phys. Lipids 141*, 72−82.
(17) Murphy, R. M. (2007) Kinetics of amyloid formation and membrane interaction with amyloidogenic proteins. *Biochim. Biophys. Acta 1768*, 1923−1934.
(18) Epand, R. M., Shai, Y., Segrest, J. P., and Anantharamaiah, G. M. (1995) Mechanisms for the modulation of membrane bilayer properties by amphipathic helical peptides. *Biopolymers 37*, 319−338.
(19) Zhu, M., Li, J., and Fink, A. L. (2003) The association of α-synuclein with membranes affects bilayer structure, stability, and fibril formation. *J. Biol. Chem. 278*, 40186−40197.
(20) Lau, T. L., Ambroggio, E. E., Tew, D. J., Cappai, R., Masters, C. L., Fidelio, G. D., Barnham, K. J., and Separovic, F. (2006) Amyloid-β peptide disruption of lipid membranes and the effect of metal ions. *J. Mol. Biol. 356*, 759−770.
(21) Krueger-Koplin, R. D., Sorgen, P. L., Krueger-Koplin, S. T., Rivera-Torres, I. O., Cahill, S. M., Hicks, D. B., Grinius, L., Krulwich, T. A., and Girvin, M. E. (2004) An evaluation of detergents for NMR structural studies of membrane proteins. *J. Biomol. NMR 28*, 43−57.
(22) Mishraa, V. K., Palgunachari, M. N., Anantharamaiah, G. M., Jones, M. K., Segrest, J. P., and Krishna, N. R. (2001) Solution NMR structure of a model class A (apolipoprotein) amphipathic α helical peptide. *Peptides 22*, 567−573.
(23) Thuau, R., Guilhaudis, L., Segalas-Milazzo, I., Chartrel, N., Oulyadi, H., Boivin, S., Fournier, A., Leprince, J., Davoust, D., and Vaudry, H. (2005) Structural studies on 26RFa, a novel human RFamide-related peptide with orexigenic activity. *Peptides 26*, 779−789.
(24) Resende, J. M., Moraes, C. M., Prates, M. V., Cesar, A., Almeida, F. C., Mundim, N. C., Valente, A. P., Bemquerer, M. P., Pilo-Veloso, D., and Bechinger, B. (2008) Solution NMR structures of the antimicrobial peptides phylloseptin-1, -2, and -3 and biological activity: The role of charges and hydrogen bonding interactions in stabilizing helix conformations. *Peptides 29*, 1633−1644.
(25) Munishkina, L. A., Phelan, C., Uversky, V. N., and Fink, A. L. (2003) Conformational behavior and aggregation of α-synuclein in organic solvents: Modeling the effects of membranes. *Biochemistry 42*, 2720−2730.
(26) Uversky, V. N. (2009) Intrinsically disordered proteins and their environment: Effects of strong denaturants, temperature, pH, counter ions, membranes, binding partners, osmolytes, and macromolecular crowding. *Protein J. 28*, 305−325.
(27) Piotto, M., Saudek, V., and Sklenar, V. (1992) Gradient-tailored excitation for single-quantum NMR spectroscopy of aqueous solutions. *J. Biomol. NMR 2*, 661−665.
(28) Delaglio, F., Grzesiek, S., Vuister, G. W., Zhu, G., Pfeifer, J., and Bax, A. (1995) NMRPipe: A multidimensional spectral processing system based on UNIX pipes. *J. Biomol. NMR 6*, 277−293.
(29) Goddard, T. D., and Kneller, D. G. (2008) *SPARKY 3*, University of California, San Francisco.
(30) Brunger, A. T., Adams, P. D., Clore, G. M., DeLano, W. L., Gros, P., Grosse-Kunstleve, R. W., Jiang, J. S., Kuszewski, J., Nilges, M., Pannu, N. S., Read, R. J., Rice, L. M., Simonson, T., and Warren, G. L. (1998) Crystallography & NMR system: A new software suite for macromolecular structure determination. *Acta Crystallogr. D54*, 905−921.
(31) Laskowski, R. A., Rullmannn, J. A., MacArthur, M. W., Kaptein, R., and Thornton, J. M. (1996) AQUA and PROCHECK-NMR: Programs for checking the quality of protein structures solved by NMR. *J. Biomol. NMR 8*, 477−486.
(32) Koradi, R., Billeter, M., and Wüthrich, K. (1996) MOLMOL: A program for display and analysis of macromolecular structures. *J. Mol. Graphics 14*, 29−32 , 51−55.
(33) Yang, J. T., Wu, C. S., and Martinez, H. M. (1986) Calculation of protein conformation from circular dichroism. *Methods Enzymol. 130*, 208−269.
(34) Wishart, D. S., Sykes, B. D., and Richards, F. M. (1991) Relationship between nuclear magnetic resonance chemical shift and protein secondary structure. *J. Mol. Biol. 222*, 311−333.
(35) Wishart, D. S., and Sykes, B. D. (1994) Chemical shifts as a tool for structure determination. *Methods Enzymol. 239*, 363−392.
(36) Merutka, G., Dyson, H. J., and Wright, P. E. (1995) 'Random coil' $^{1}$H chemical shifts obtained as a function of temperature and trifluoroethanol concentration for the peptide series GGXGG. *J. Biomol. NMR 5*, 14−24.
(37) Wüthrich, K. (1986) *NMR of Proteins and Nucleic Acids*, John Wiley & Sons, New York.
(38) Yip, C. M., Darabie, A. A., and McLaurin, J. (2002) Aβ42-peptide assembly on lipid bilayers. *J. Mol. Biol. 318*, 97−107.
(39) Necula, M., Chirita, C. N., and Kuret, J. (2003) Rapid anionic micelle-mediated α-synuclein fibrillization in vitro. *J. Biol. Chem. 278*, 46674−46680.
(40) Chirita, C. N., Necula, M., and Kuret, J. (2003) Anionic micelles and vesicles induce tau fibrillization in vitro. *J. Biol. Chem. 278*, 25644−25650.
(41) Zhu, M., and Fink, A. L. (2003) Lipid binding inhibits α-synuclein fibril formation. *J. Biol. Chem. 278*, 16873−16877.
(42) Sharp, J. S., Forrest, J. A., and Jones, R. A. (2002) Surface denaturation and amyloid fibril formation of insulin at model lipid-water interfaces. *Biochemistry 41*, 15810−15819.
(43) Sabate, R., and Estelrich, J. (2005) Stimulatory and inhibitory effects of alkyl bromide surfactants on β-amyloid fibrillogenesis. *Langmuir 21*, 6944−6949.
(44) Abedini, A., and Raleigh, D. P. (2009) A role for helical intermediates in amyloid formation by natively unfolded polypeptides? *Phys. Biol. 6*, 015005.
(45) Uversky, V. N. (2008) Amyloidogenesis of natively unfolded proteins. *Curr. Alzheimer Res. 5*, 260−287.
(46) Liu, G., Prabhakar, A., Aucoin, D., Simon, M., Sparks, S., Robbins, K. J., Sheen, A., Petty, S. A., and Lazo, N. D. (2010) Mechanistic studies of peptide self-assembly: Transient α-helices to stable β-sheets. *J. Am. Chem. Soc. 132*, 18223−18232.
(47) Munishkina, L. A., Fink, A. L., and Uversky, V. N. (2004) Conformational prerequisites for formation of amyloid fibrils from histones. *J. Mol. Biol. 342*, 1305−1324.
(48) Chirita, C. N., Congdon, E. E., Yin, H., and Kuret, J. (2005) Triggers of full-length tau aggregation: A role for partially folded intermediates. *Biochemistry 44*, 5862−5872.
(49) Fink, A. L. (2006) The aggregation and fibrillation of α-synuclein. *Acc. Chem. Res. 39*, 628−634.